

# Evidence for non-exponential $pp$ $d\sigma/dt$ at low $t$ and $\sqrt{s} = 8$ TeV by TOTEM

T. Csörgő for the TOTEM Collaboration

Wigner Research Center for Physics, Budapest, Hungary  
KRF, Gyöngyös, Hungary

Introduction

Experimental setup

Event selection

LHC Optics

Data analysis

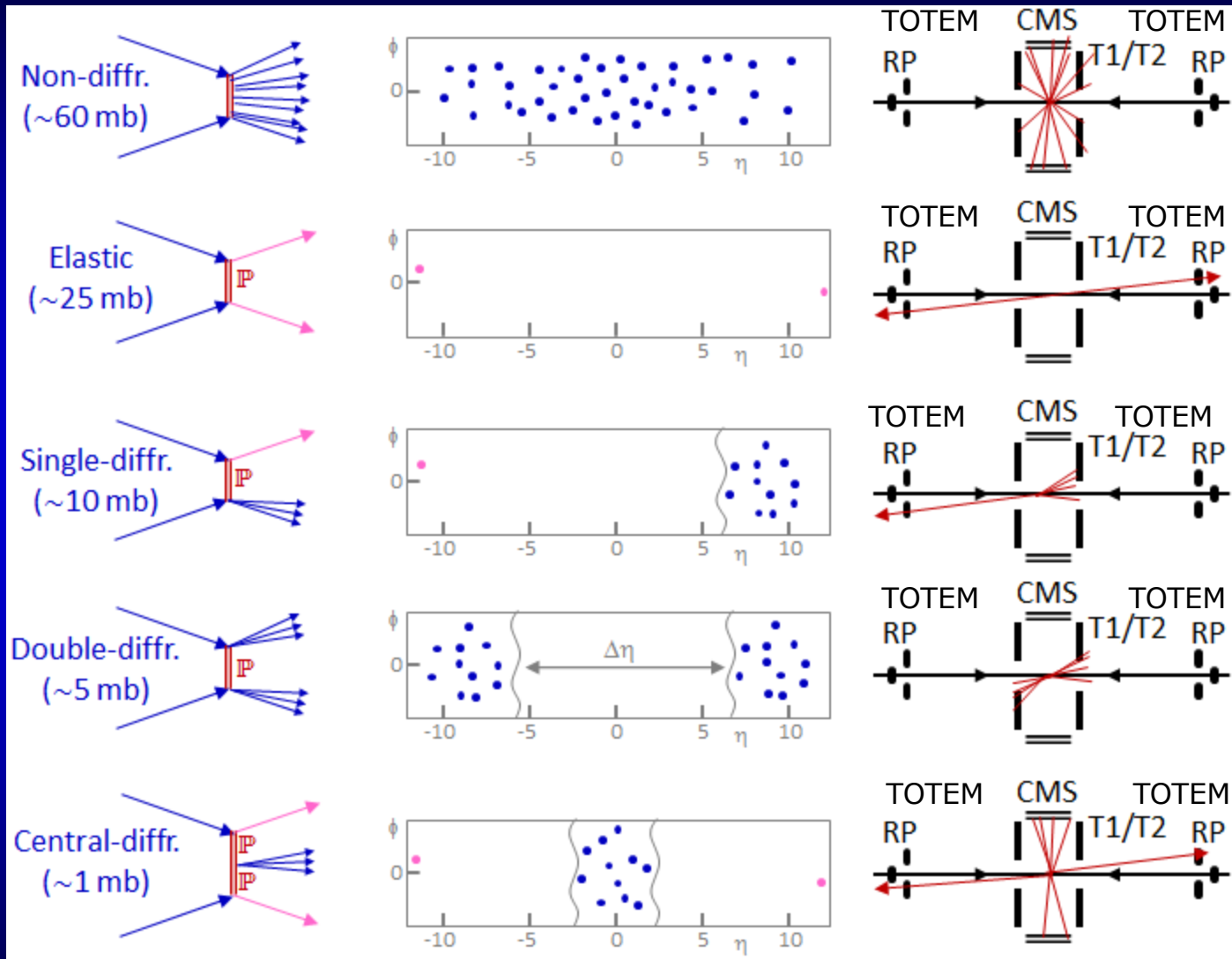
Results and cross-checks

Outlook

Summary

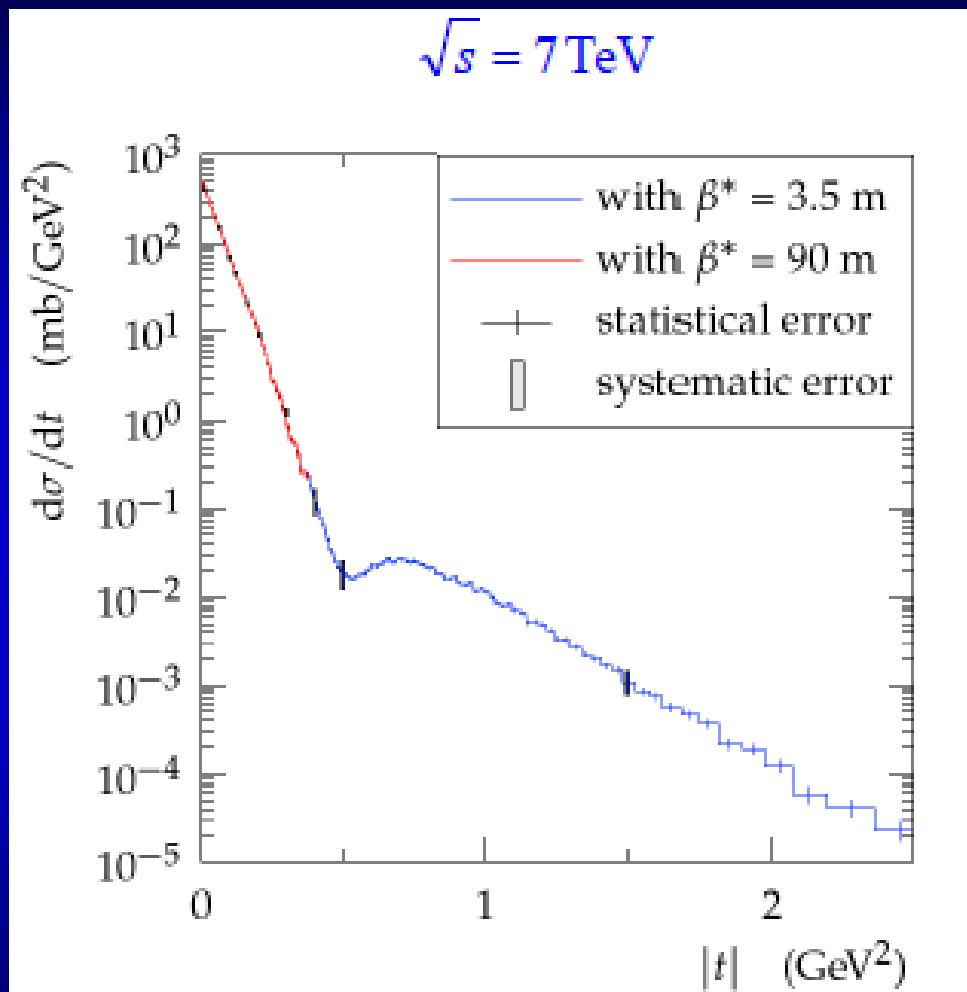


# TOTEM physics at LHC



Elastic and diffractive scattering: colorless exchange

# Earlier results on elastic scattering



Earlier hints on non-exponential behaviour:

at ISR: 21.5 to 52.8 GeV,  
change of slope  
and better fits with  
 $\exp(-B |t| - C t^2)$

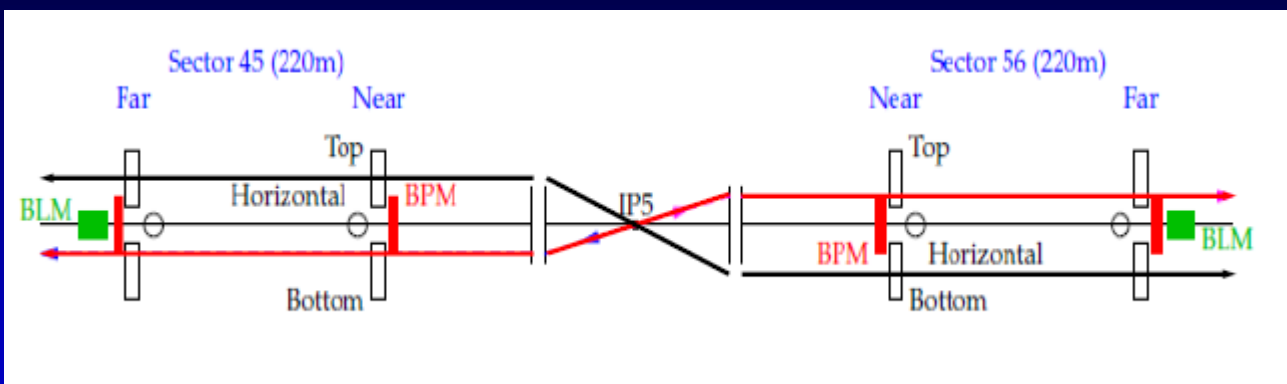
at SppS:  
Change of slope only, at  
 $|t| \sim 0.14 \text{ GeV}^2$

At Tevatron,  
non-exponential not seen

earlier LHC data  $\sim$  exponential, satisfactory fits with  $\exp(-B |t|)$ .  
New TOTEM data at low  $|t|$ : evidence for non-exponential



# RP stations for elastic scattering



Near(214 m) and Far(220 m) TOTEM RP units  
on both sides of IP5

Three RP-s in each unit:  
(top, horizontal, bottom)

Each RP:

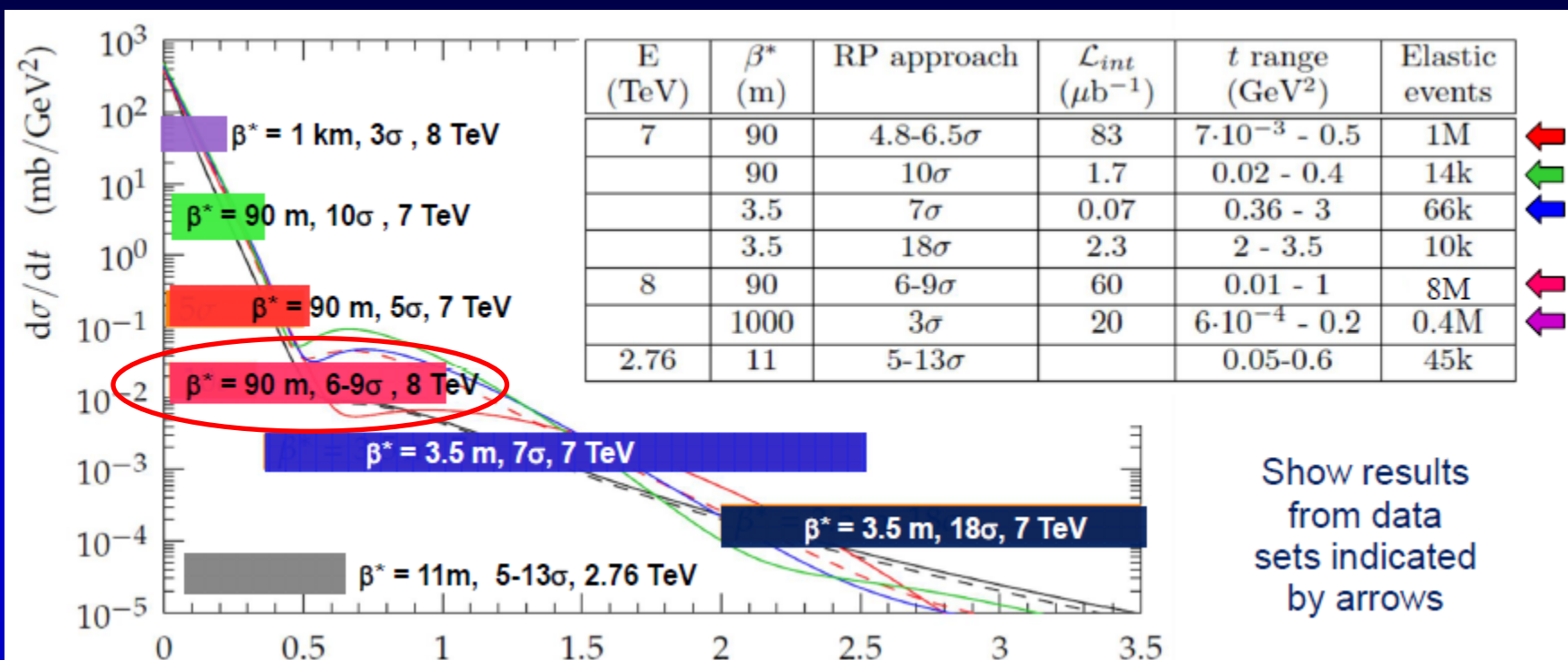
Stack of 10 silicon strips (pitch  $66 \mu\text{m}$ )

„edgeless” (active in  $\text{few} \times 10 \mu\text{m}$ )

Trigger capable electronics

Elastic scattering: two anti-parallel protons  
→ two topologies, analyzed independently:  
→ 45 bottom-56 top, 45 top-56 bottom

# TOTEM data taking

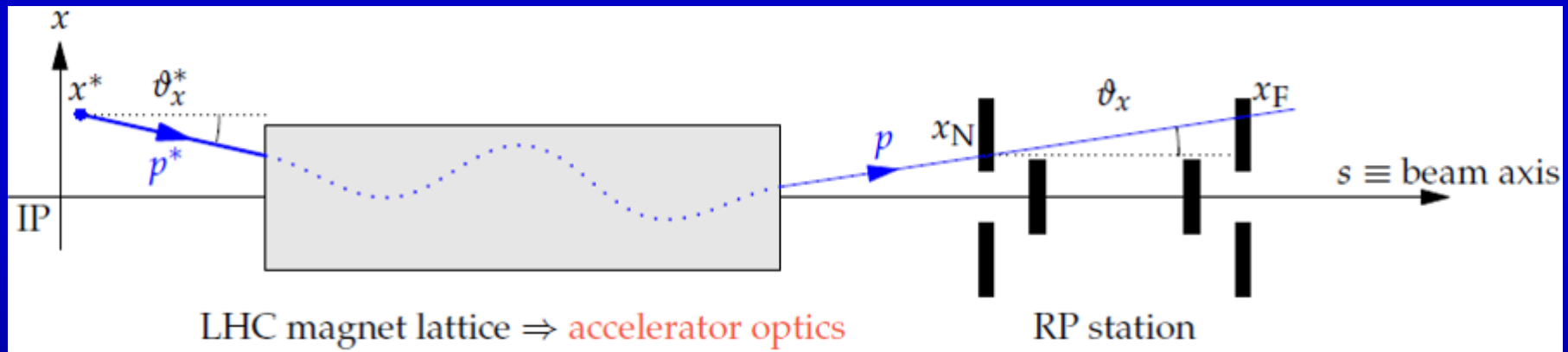
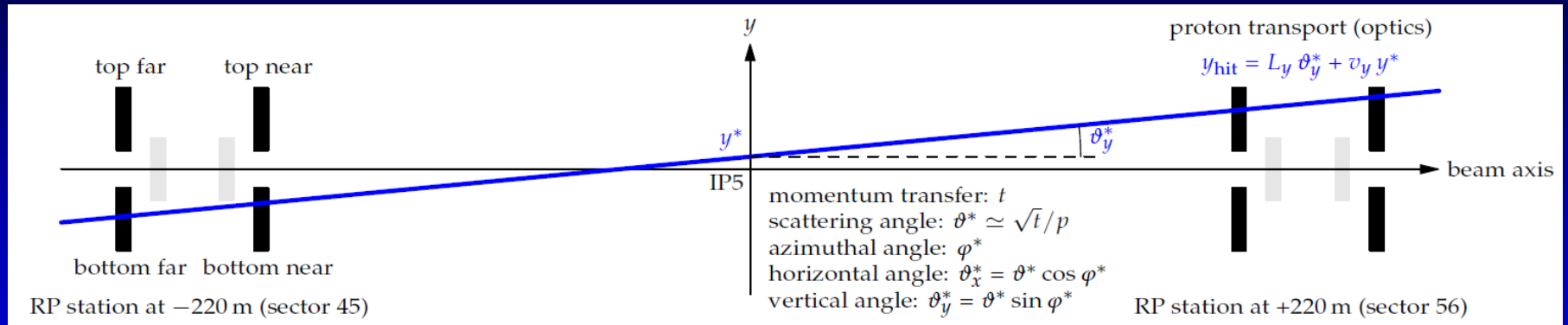


Show results from data sets indicated by arrows

July 2012 data, **special** LHC run ,  $\beta^* = 90$  m,  $\sqrt{s} = 8$  TeV

2  $\rightarrow$  3 colliding bunch pair,  $8 \times 10^{10}$  p/bunch  
 Instantaneous  $L \sim 10^{28} \text{ cm}^{-2}\text{s}^{-1}$   
 11 h data taking, RP-s at  $9.5 \sigma_{\text{beam}}$   
 Integrated  $L \sim 735 \mu\text{b}^{-1}$   
 $7.2 \cdot 10^6$  elastic events

# LHC Optics for Elastic pp Scattering



$$\begin{pmatrix} x \\ \Theta_x \\ y \\ \Theta_y \\ \Delta p/p \end{pmatrix} = \begin{pmatrix} v_x & L_x & 0 & 0 & D_x \\ v'_x & L'_x & 0 & 0 & D'_x \\ 0 & 0 & v_y & L_y & 0 \\ 0 & 0 & v'_y & L'_y & 0 \\ 0 & 0 & 0 & 0 & 1 \end{pmatrix} \begin{pmatrix} x^* \\ \Theta_x^* \\ y^* \\ \Theta_y^* \\ \Delta p/p \end{pmatrix}$$

Precise  $\sigma_{\text{tot}}$  and  $d\sigma/dt$  determination by TOTEM needs excellent control of LHC optics from data

# LHC Optics Determination, $\beta^* = 90$ m

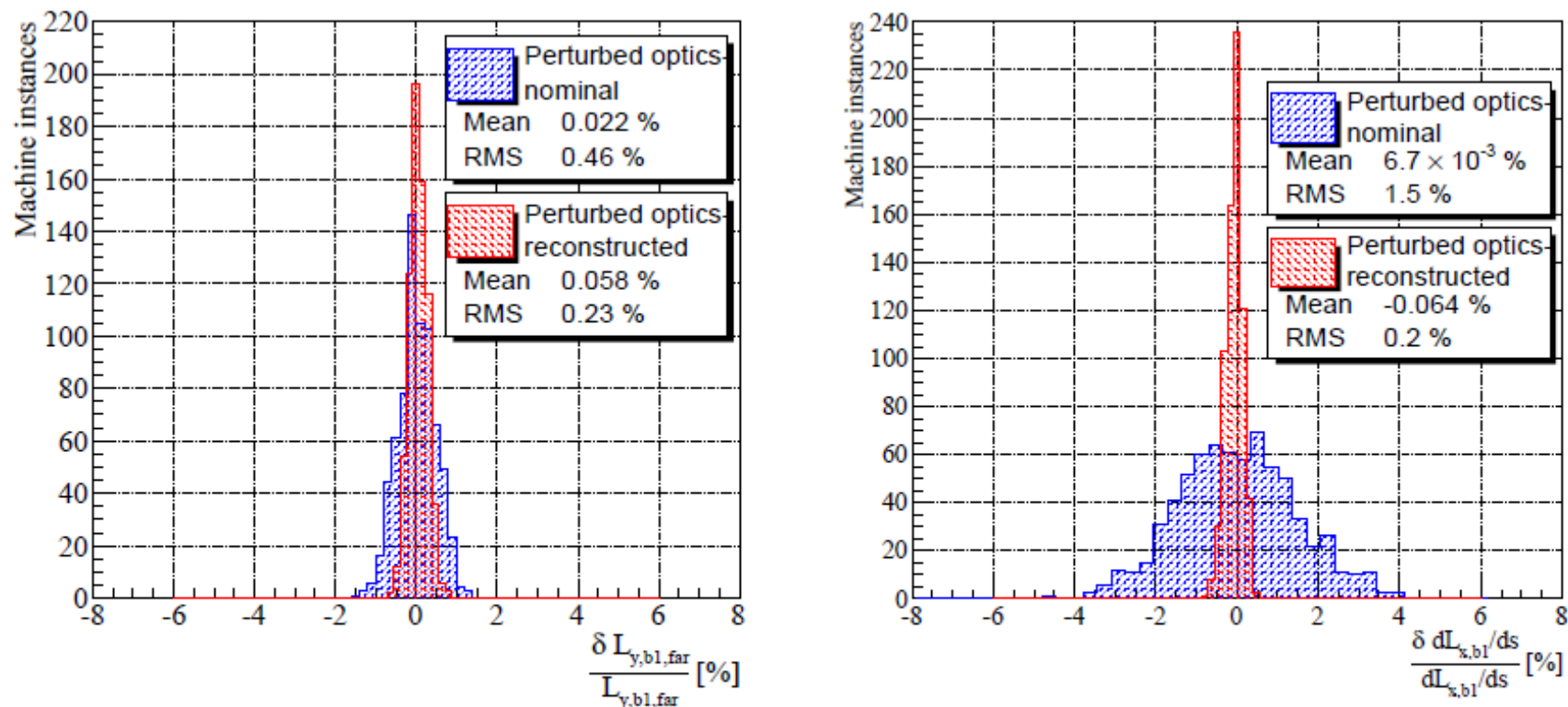


Figure 12. (color online) The MC error distribution of  $\beta^* = 90$  m optical functions  $L_y$  and  $dL_x/ds$  for Beam 1 at  $E = 4$  TeV, before and after optics estimation.

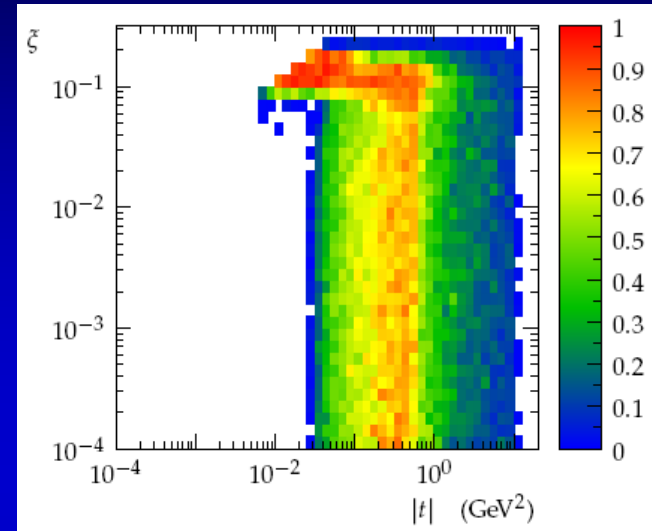
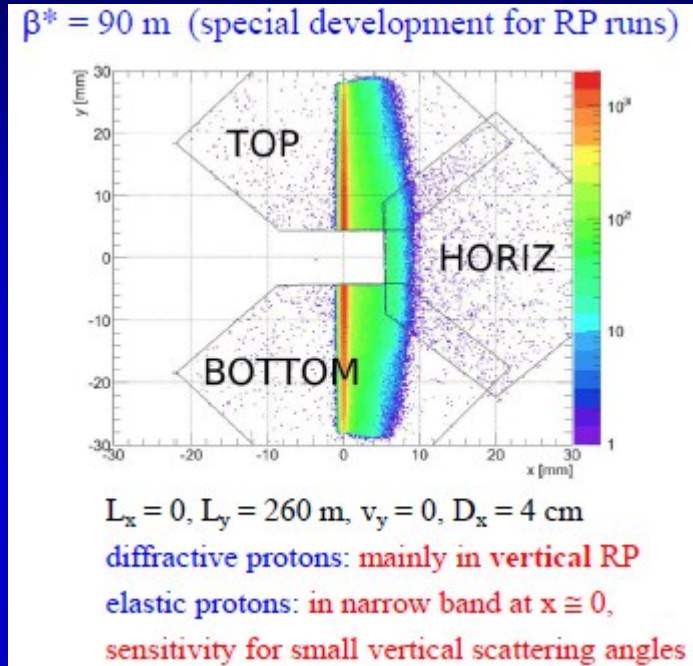
Precise control of LHC imperfections with perturbed LHC optics and recalibration from data at IP5: factors of 2 - 10

[arXiv:1406.0546](https://arxiv.org/abs/1406.0546)

# LHC optics and proton acceptance

$t = -p^2 \theta_*^2$ : four-momentum transfer squared;

$\xi = \Delta p/p$ : fractional momentum loss

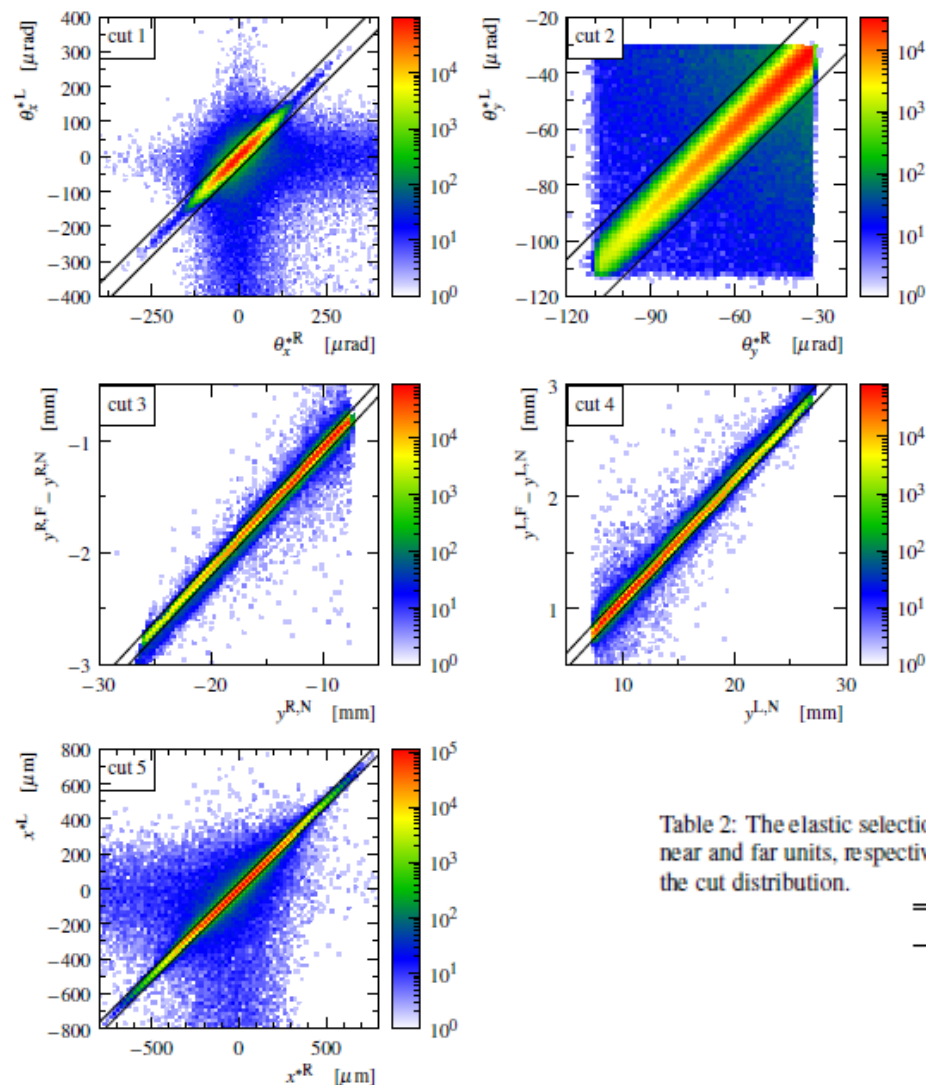


$\beta^* = 90$  m MC simulation shown  
 Parallel to point focussing,  $v_y \sim 0$   
 Large effective length  $L_y$   
 Elastic scattering events: in vertical RPs

$\beta^* = 90$  m  
 Diffraction:  
 all  $\xi$  if  $|t| \geq 10^{-2}$  GeV<sup>2</sup>,  
 soft & semi-hard diffr.  
 Elastic: low to mid  $|t|$   
 Total cross-section

RP unit	$L_x$	$v_x$	$L_y$	$v_y$
near	2.45 m	-2.17	239 m	0.040
far	-0.37 m	-1.87	264 m	0.021

# Kinematic cuts: selection of elastics

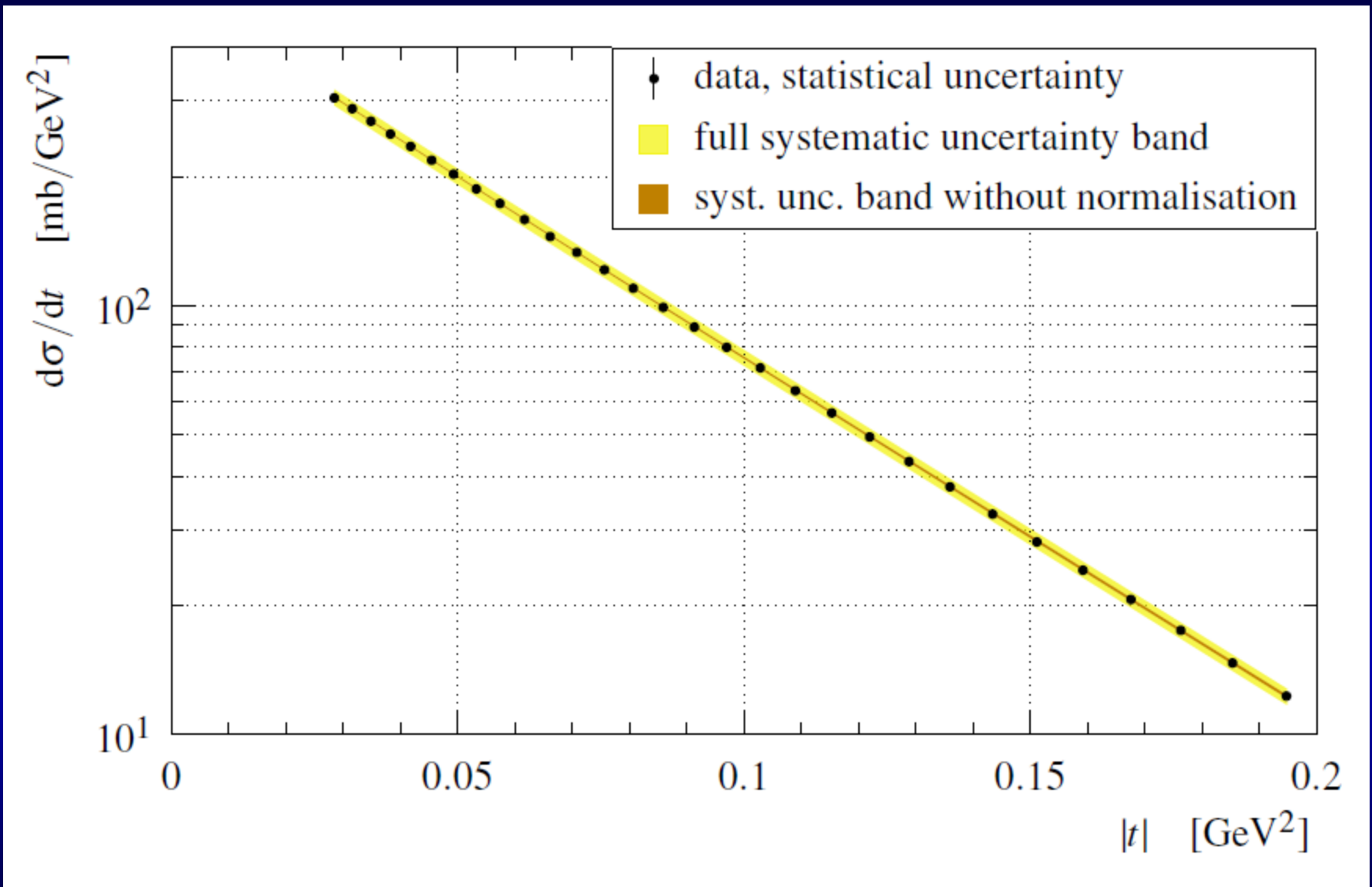


Precise control of LHC optics  
and elastic scattering:  
Kinematics reconstruction  
Alignment  
Optics recalibration  
Resolution unfolding  
Acceptance correction  
Background subtraction  
Detection & efficiency  
Angular resolution  
Normalization  
Binning

Table 2: The elastic selection cuts. The superscripts R and L refer to the right and left arm, N and F correspond to the near and far units, respectively. The constant  $\alpha = L_y^F/L_y^N - 1 \approx 0.11$ . The right-most column gives a typical RMS of the cut distribution.

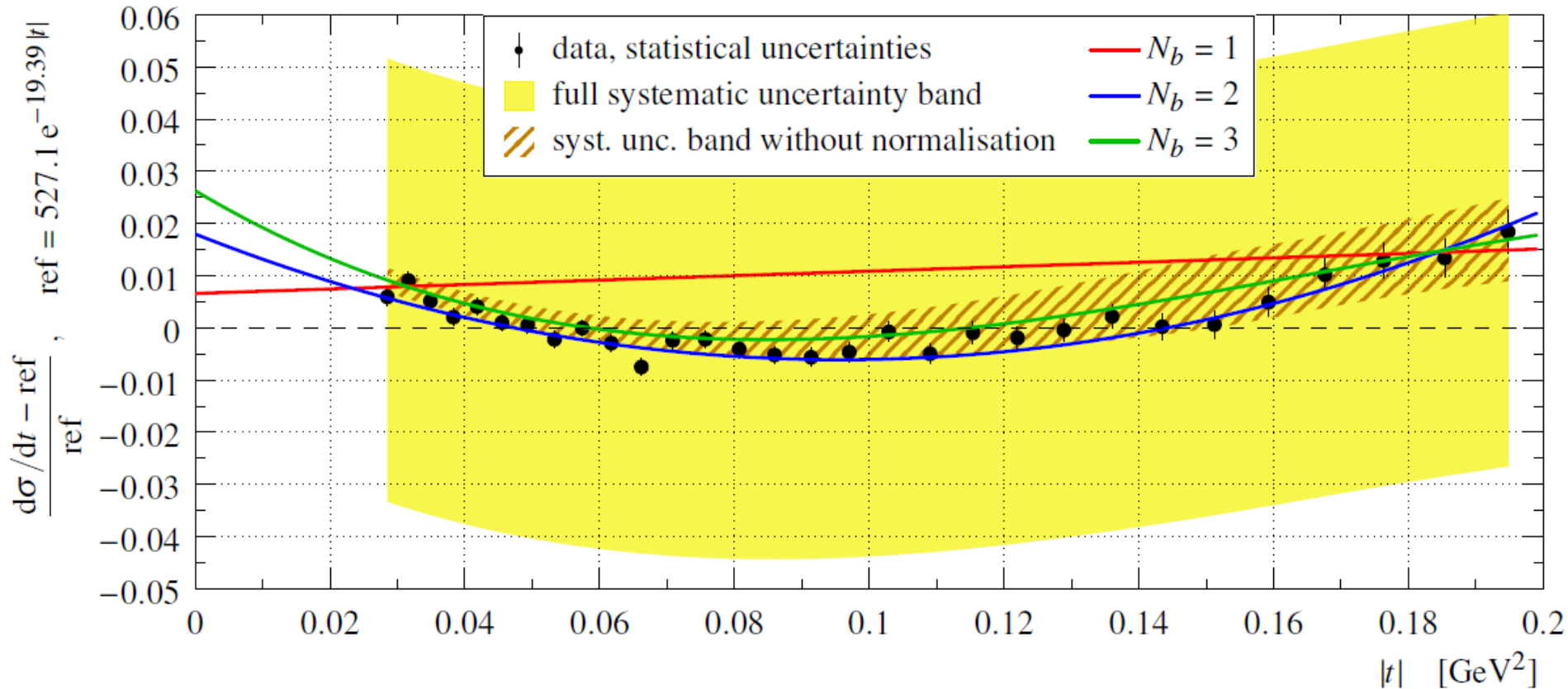
discriminator	cut quantity	RMS ( $\equiv 1\sigma$ )
1	$\theta_x^R - \theta_x^L$	$9.5 \mu\text{rad}$
2	$\theta_y^R - \theta_y^L$	$3.3 \mu\text{rad}$
3	$\alpha y^{R,N} - (y^{R,F} - y^{R,N})$	$18 \mu\text{m}$
4	$\alpha y^{L,N} - (y^{L,F} - y^{L,N})$	$18 \mu\text{m}$
5	$x^{R} - x^{L}$	$8.5 \mu\text{m}$

# Differential cross-section @ 8 TeV



$t = -p^2 \theta_*^2$ ; „optimized binning”; almost exponential but if one looks in detail, NOT

# Differential cross-section @ 8 TeV



$$\frac{d\sigma}{dt}(t) = \frac{d\sigma}{dt} \Big|_{t=0} \exp\left(\sum_{i=1}^{N_b} b_i t^i\right),$$

$$\chi^2 = \Delta^T V^{-1} \Delta,$$

$$V = V_{\text{stat}} + V_{\text{syst}}$$

$$\Delta_i = \frac{d\sigma}{dt} \Big|_{\text{bin } i} - \frac{1}{\Delta t_i} \int_{\text{bin } i} f(t) dt,$$

$N_b = 1$  fits excluded. Relative to best exponential, a significant  $7.2\sigma$  deviation found.

# Differential cross-section @ 8 TeV

Table 4: Details of the fits in Figure 11 using parametrisation Eq. (15). The matrices give the correlation factors between the fit parameters.

$N_b$	$d\sigma/dt _{t=0}$ [mb/GeV <sup>2</sup> ]	$b_1$ [GeV <sup>-2</sup> ]	$b_2$ [GeV <sup>-4</sup> ]	$b_3$ [GeV <sup>-6</sup> ]	$\chi^2/\text{ndf}$	p-value	significance
1	$531 \pm 22$ $\begin{pmatrix} +1.00 & -0.11 \\ -0.11 & +1.00 \end{pmatrix}$	$-19.35 \pm 0.06$	-	-	$117.5/28 = 4.20$	$6.2 \cdot 10^{-13}$	$7.20 \sigma$
2	$537 \pm 22$ $\begin{pmatrix} +1.00 & +0.19 & -0.34 \\ +0.19 & +1.00 & -0.76 \\ -0.34 & -0.76 & +1.00 \end{pmatrix}$	$-19.89 \pm 0.08$	$2.61 \pm 0.30$	-	$29.3/27 = 1.09$	0.35	$0.94 \sigma$
3	$541 \pm 22$ $\begin{pmatrix} +1.00 & +0.08 & -0.04 & -0.02 \\ +0.08 & +1.00 & -0.90 & +0.85 \\ -0.04 & -0.90 & +1.00 & -0.99 \\ -0.02 & +0.85 & -0.99 & +1.00 \end{pmatrix}$	$-20.14 \pm 0.15$	$5.95 \pm 1.75$	$-12.0 \pm 6.2$	$25.5/26 = 0.98$	0.49	$0.69 \sigma$

$$\frac{d\sigma}{dt}(t) = \frac{d\sigma}{dt}\Big|_{t=0} \exp\left(\sum_{i=1}^{N_b} b_i t^i\right),$$

$$\chi^2 = \Delta^T V^{-1} \Delta,$$

$$V = V_{\text{stat}} + V_{\text{syst}}$$

$$\Delta_i = \frac{d\sigma}{dt}\Big|_{\text{bin } i} - \frac{1}{\Delta t_i} \int_{\text{bin } i} f(t) dt,$$

$N_b = 1$  fits excluded. Relative to best exponential, a significant  $7.2\sigma$  deviation found.

# Cross-check: „per-mille” binnings

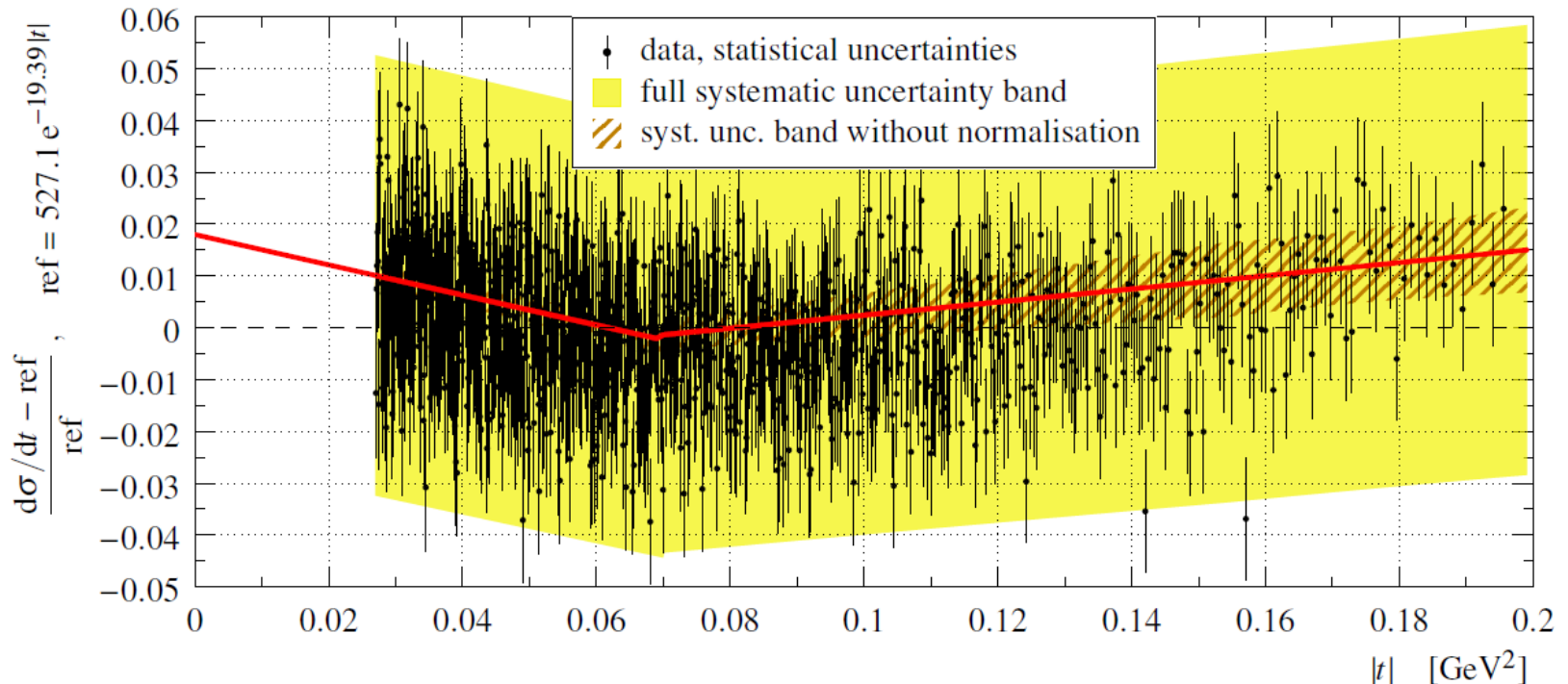


Figure 12: Differential cross-section using the “per-mille” binning and plotted as relative difference from the reference exponential (see vertical axis). The black dots represent data points with statistical uncertainty bars. The red line shows pure exponential fits in regions below and above  $|t| = 0.07 \text{ GeV}^2$ , see Eq. (19). The yellow band corresponds to the full systematic uncertainty, the brown-hatched one includes all systematic contributions except the normalisation. Both bands are centred around the fit curve.

$$\frac{d\sigma}{dt}(t) = \begin{cases} a_1 e^{b_1|t|} & |t| < 0.07 \text{ GeV}^2 \\ a_2 e^{b_2|t|} & |t| > 0.07 \text{ GeV}^2 \end{cases}$$

$$\chi_p^2 = \Delta_p^T V_p^{-1} \Delta_p, \quad \Delta_p = \begin{pmatrix} a_1 - a_2 \\ b_1 - b_2 \end{pmatrix}$$

Simple exp fits excluded. Different binnings show the same effect. Here  $7.8 \sigma$  significance.

# Systematics

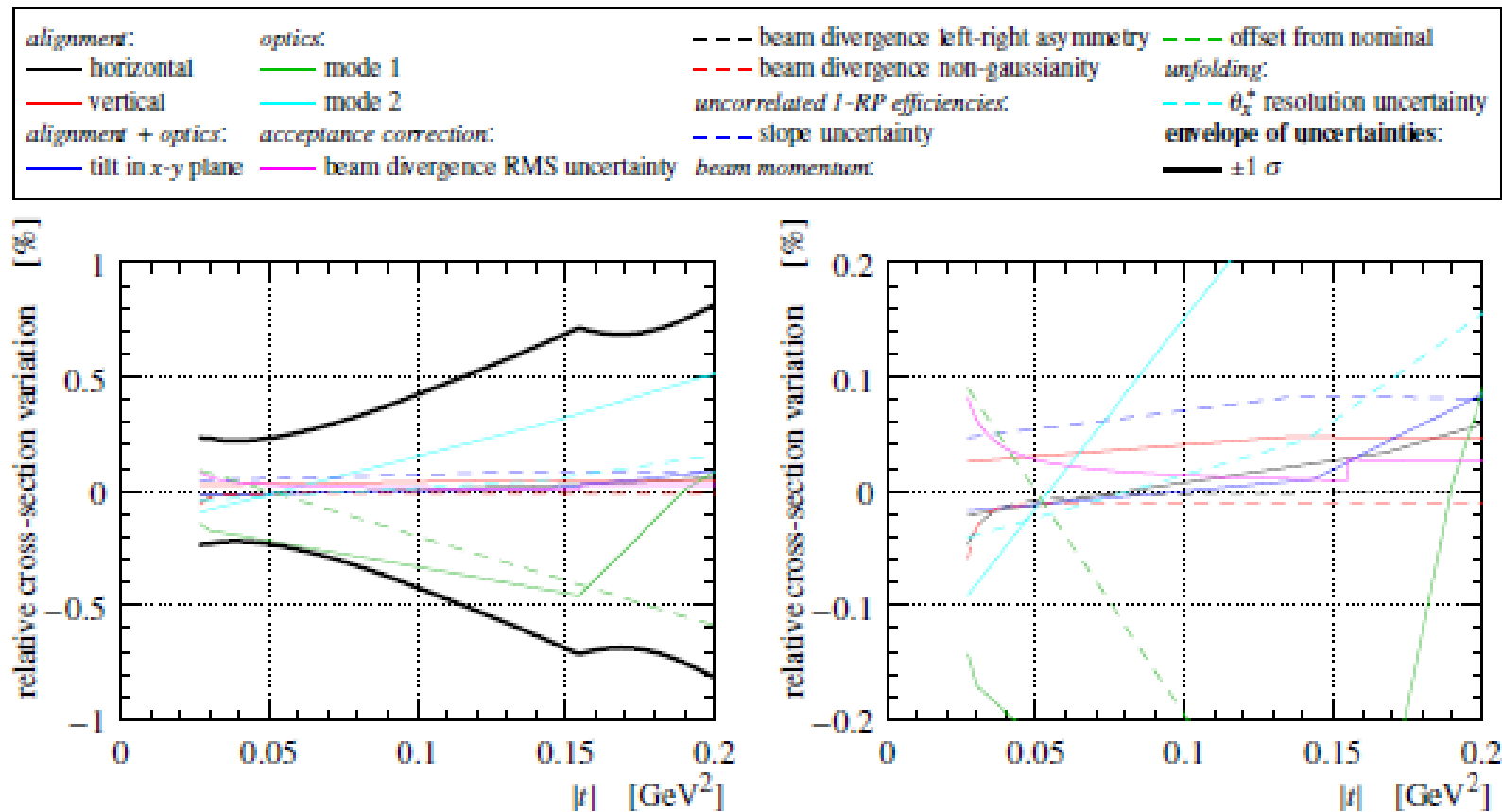


Figure 9: Impact of  $t$ -dependent systematic effects on the differential cross-section. Each curve corresponds to a systematic error at  $1 \sigma$ , cf. Eq. (13). The two contributions due to optics correspond to the two vectors in Eq. (8). The envelope is determined by summing all shown contributions in quadrature for each  $|t|$  value. The right-hand plot provides a vertical zoom; note that the envelope is out of scale.

No significant effect found on the total pp cross-section,  $\sigma_{\text{tot}}$

# „Blessed“ TOTEM physics result

Special TOTEM run probing into the Coulomb-nuclear interference region

Measurement down to  $|t| \sim 6 \times 10^{-4} \text{ GeV}^2$ :

- $\beta^* = 1000 \text{ m}$  optics
- Roman Pot approach to  $3 \sigma$  from the beam centre

$$F^{C+H} = F^C + F^H e^{i\alpha\Psi}$$

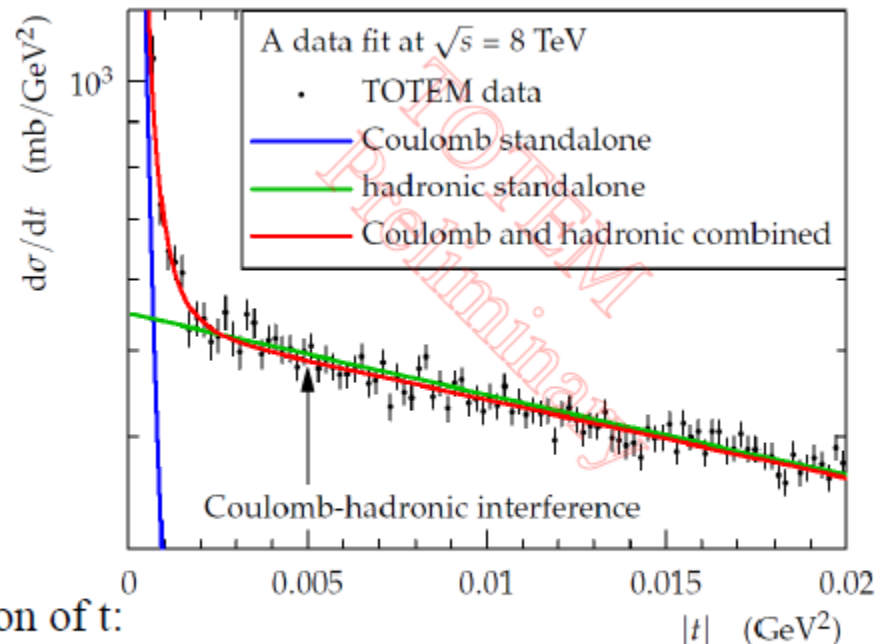
$$|F^H| \arg(F^H)$$

$$A e^{-B(t)|t|}$$

hadronic phase as function of  $t$ :

implications on behaviour of elastic scattering in impact parameter space

preferentially central or peripheral ?



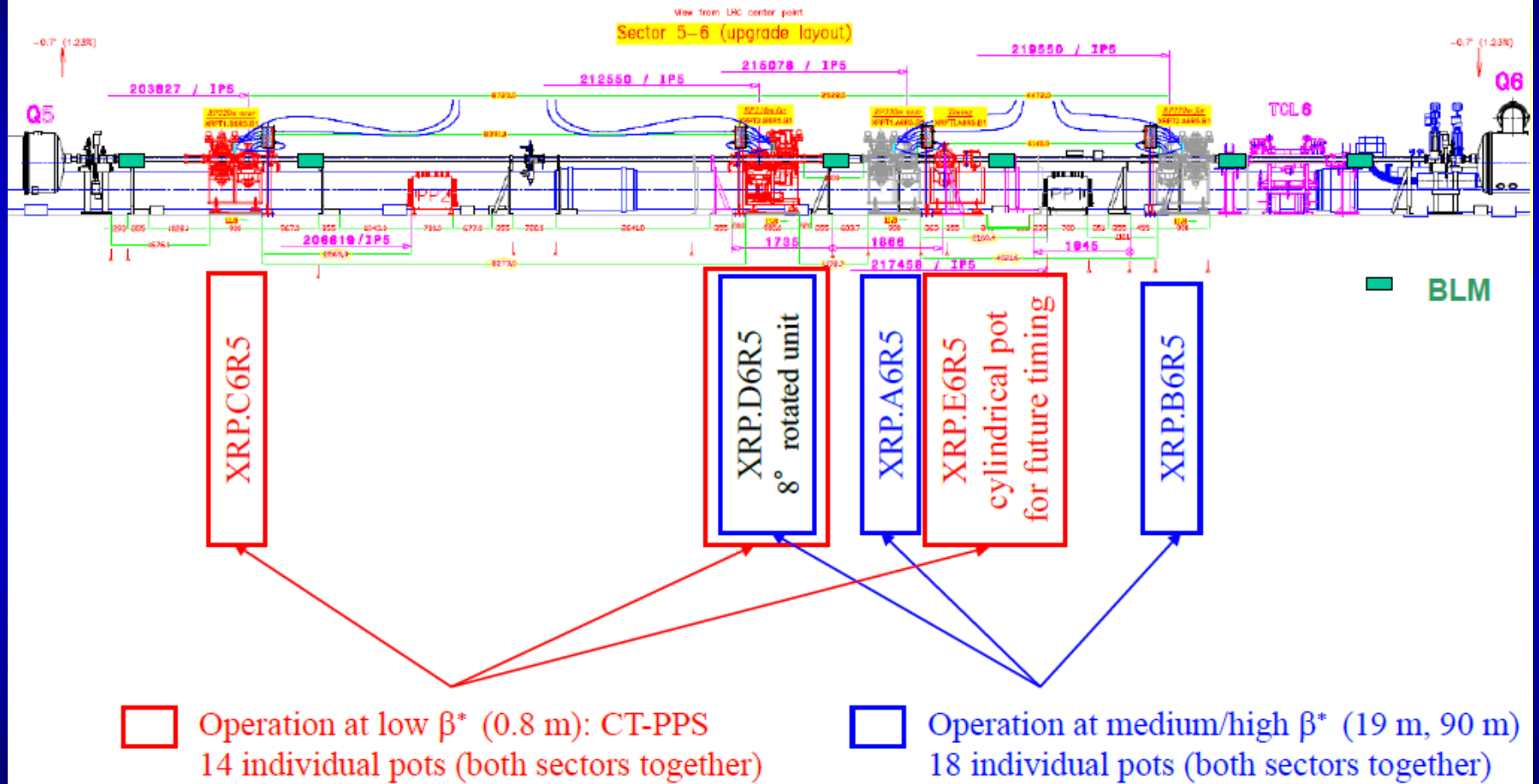
Combined 1 km and 90 m data: exclude simplified West-Yennie interference formula (requires constant B)

Confirms earlier  $\sigma_{\text{tot}}$  measurements

Constrains impact parameter picture of pp collisions

# TOTEM status after LS1

26 Roman Pots: the largest Roman Pot system ever operated at a collider



All RP insertions successful so far. Standalone operations as well as common runs with CMS.  
For more details see M. Deile's talk at LHCC, Sept 2015.

# Summary

Nucl. Phys. B899 (2015) 297 by TOTEM:  
low- $|t|$   $d\sigma/dt$  for elastic pp at  $\sqrt{s} = 8$  TeV  
with unprecedented precision

Significantly non-exponential behaviour  
more than  $7 \sigma$  effect -  
protons are non-Gaussian in  $b$

No significant effect on earlier  
 $\sigma_{\text{tot}}$  measurements at 8 TeV

New results on Coulomb-nuclear  
at even lower  $t$  approved.

First data taking at 13 TeV

# The TOTEM Collaboration

## The TOTEM Collaboration

G. Antchev<sup>1</sup>, P. Aspell<sup>q</sup>, I. Atanassov<sup>1</sup>, V. Avati<sup>q</sup>, J. Baechler<sup>q</sup>, V. Berardi<sup>ji</sup>, M. Berretti<sup>q,o</sup>, E. Bossini<sup>o</sup>, U. Bottigli<sup>o</sup>, M. Bozzo<sup>1</sup>, P. Broulma<sup>a</sup>, A. Buzzo<sup>1</sup>, F. S. Cafagna<sup>1</sup>, C. E. Campanella<sup>ki</sup>, M. G. Catanesi<sup>1</sup>, M. Csanád<sup>g,2</sup>, T. Csörgő<sup>g,h</sup>, M. Deile<sup>q</sup>, F. De Leonardis<sup>ki</sup>, A. D'Orazio<sup>ki</sup>, M. Doubek<sup>c</sup>, K. Eggert<sup>f</sup>, V. Eremin<sup>5</sup>, F. Ferro<sup>1</sup>, A. Fiergolski<sup>i,4</sup>, F. Garcia<sup>e</sup>, V. Georgiev<sup>a</sup>, S. Giani<sup>q</sup>, L. Grzanka<sup>p,3</sup>, C. Guaragnella<sup>ki</sup>, J. Hammerbauer<sup>a</sup>, J. Heino<sup>e</sup>, A. Karev<sup>q</sup>, J. Kašpar<sup>b,q</sup>, J. Kopal<sup>b</sup>, V. Kunderát<sup>b</sup>, S. Lami<sup>o</sup>, G. Latino<sup>o</sup>, R. Lauhakangas<sup>e</sup>, R. Linhart<sup>a</sup>, E. Lippmaa<sup>d</sup>, J. Lippmaa<sup>d</sup>, M. V. Lokajčiček<sup>b</sup>, L. Losurdo<sup>o</sup>, M. Lo Vetere<sup>m,1</sup>, F. Lucas Rodríguez<sup>q</sup>, M. Macrì<sup>l</sup>, A. Mercadante<sup>1</sup>, N. Minafra<sup>qj</sup>, S. Minutoli<sup>1</sup>, T. Naaranoja<sup>e,f</sup>, F. Nemes<sup>g,2</sup>, H. Niewiadomski<sup>f</sup>, E. Oliveri<sup>q</sup>, F. Oljemark<sup>e,f</sup>, R. Orava<sup>e,f</sup>, M. Oriunno<sup>6</sup>, K. Österberg<sup>e,f</sup>, P. Palazzi<sup>q</sup>, L. Paločko<sup>a</sup>, V. Passaro<sup>ki</sup>, Z. Peroutka<sup>a</sup>, V. Petruzzelli<sup>ki</sup>, T. Politi<sup>ki</sup>, J. Procházka<sup>b</sup>, F. Prudeniano<sup>ki</sup>, M. Quinto<sup>ij</sup>, E. Radermacher<sup>q</sup>, E. Radicioni<sup>i</sup>, F. Ravotti<sup>q</sup>, E. Robutti<sup>1</sup>, L. Ropelewski<sup>q</sup>, G. Ruggiero<sup>q</sup>, H. Saarikko<sup>e,f</sup>, A. Scribano<sup>o</sup>, J. Smajek<sup>q</sup>, W. Snoeys<sup>q</sup>, T. Sodzawiczny<sup>q</sup>, J. Sziklai<sup>g</sup>, C. Taylor<sup>f</sup>, N. Turini<sup>o</sup>, V. Vacek<sup>c</sup>, J. Welti<sup>e,f</sup>, P. Wyszkowski<sup>p</sup>, K. Zielinski<sup>p</sup>

<sup>a</sup>University of West Bohemia, Pilsen, Czech Republic.

<sup>b</sup>Institute of Physics of the Academy of Sciences of the Czech Republic, Praha, Czech Republic.

<sup>c</sup>Czech Technical University, Praha, Czech Republic.

<sup>d</sup>National Institute of Chemical Physics and Biophysics NICPB, Tallinn, Estonia.

<sup>e</sup>Helsinki Institute of Physics, Helsinki, Finland.

<sup>f</sup>Department of Physics, University of Helsinki, Helsinki, Finland.

<sup>g</sup>Wigner Research Centre for Physics, RMKI, Budapest, Hungary.

<sup>h</sup>KRF University College, Gyöngyös, Hungary.

<sup>i</sup>INFN Sezione di Bari, Bari, Italy.

<sup>j</sup>Dipartimento Interateneo di Fisica di Bari, Bari, Italy.

<sup>k</sup>Dipartimento di Ingegneria Elettrica e dell'Informazione - Politecnico di Bari, Bari, Italy.

<sup>l</sup>INFN Sezione di Genova, Genova, Italy.

<sup>m</sup>Università degli Studi di Genova, Italy.

<sup>n</sup>INFN Sezione di Pisa, Pisa, Italy.

<sup>o</sup>Università degli Studi di Siena and Gruppo Collegato INFN di Siena, Siena, Italy.

<sup>p</sup>AGH University of Science and Technology, Krakow, Poland.

<sup>q</sup>CERN, Geneva, Switzerland.

<sup>r</sup>Case Western Reserve University, Dept. of Physics, Cleveland, OH, USA.

8  
countries  
18  
institutions  
85  
people

Thank you!

# Backup slides – Questions?

# Backup slide – covariance matrix

Table 3: The elastic differential cross-section as determined in this analysis using the “optimised” binning. The three left-most columns describe the bins in  $t$ . The representative point gives the  $t$  value suitable for fitting [23]. The other columns are related to the differential cross-section. The four right-most columns give the leading systematic biases in  $d\sigma/dt$  for  $1\sigma$ -shifts in the respective quantities,  $\delta s_q$ , see Eqs. (13) and (14). The two contributions due to optics correspond to the two vectors in Eq. (8).

$ t $ bin [GeV <sup>2</sup> ]			$d\sigma/dt$ [mb/GeV <sup>2</sup> ]						
left edge	right edge	represent. point	value	statistical uncertainty	systematic uncertainty	normalisation $N$	optics mode 1	optics mode 2	beam momentum
0.02697	0.03005	0.02850	305.09	0.527	12.85	+12.83	-0.479	-0.263	+0.257
0.03005	0.03325	0.03164	287.95	0.478	12.08	+12.06	-0.502	-0.217	+0.206
0.03325	0.03658	0.03491	269.24	0.436	11.32	+11.31	-0.491	-0.174	+0.159
0.03658	0.04005	0.03831	251.31	0.401	10.59	+10.57	-0.478	-0.135	+0.115
0.04005	0.04365	0.04184	235.15	0.371	9.874	+ 9.861	-0.465	-0.0981	+0.0750
0.04365	0.04740	0.04551	218.32	0.343	9.185	+ 9.172	-0.451	-0.0647	+0.0383
0.04740	0.05129	0.04933	202.64	0.318	8.521	+ 8.509	-0.437	-0.0343	+0.0052
0.05129	0.05534	0.05330	187.10	0.295	7.882	+ 7.870	-0.421	-0.0070	-0.0244
0.05534	0.05956	0.05743	173.06	0.274	7.270	+ 7.257	-0.405	+0.0172	-0.0504
0.05956	0.06394	0.06173	158.77	0.255	6.685	+ 6.672	-0.388	+0.0385	-0.0731
0.06394	0.06850	0.06620	144.93	0.236	6.127	+ 6.114	-0.370	+0.0569	-0.0925
0.06850	0.07324	0.07085	133.12	0.219	5.597	+ 5.584	-0.352	+0.0724	-0.109
0.07324	0.07817	0.07568	121.24	0.203	5.096	+ 5.082	-0.334	+0.0853	-0.122
0.07817	0.08329	0.08071	109.77	0.188	4.623	+ 4.609	-0.316	+0.0957	-0.132
0.08329	0.08862	0.08593	99.077	0.174	4.179	+ 4.164	-0.297	+0.104	-0.140
0.08862	0.09417	0.09137	89.126	0.161	3.762	+ 3.747	-0.279	+0.109	-0.145
0.09417	0.09994	0.09702	79.951	0.148	3.374	+ 3.359	-0.260	+0.113	-0.147
0.09994	0.10593	0.10290	71.614	0.137	3.014	+ 2.998	-0.242	+0.115	-0.148
0.10593	0.11217	0.10902	63.340	0.125	2.680	+ 2.664	-0.224	+0.115	-0.147
0.11217	0.11866	0.11538	56.218	0.115	2.373	+ 2.357	-0.206	+0.114	-0.144
0.11866	0.12540	0.12199	49.404	0.105	2.092	+ 2.075	-0.189	+0.111	-0.139
0.12540	0.13242	0.12887	43.300	0.0961	1.835	+ 1.818	-0.173	+0.107	-0.134
0.13242	0.13972	0.13602	37.790	0.0876	1.601	+ 1.585	-0.157	+0.102	-0.127
0.13972	0.14730	0.14346	32.650	0.0795	1.391	+ 1.374	-0.142	+0.0974	-0.120
0.14730	0.15520	0.15120	28.113	0.0720	1.201	+ 1.185	-0.127	+0.0924	-0.112
0.15520	0.16340	0.15925	24.155	0.0659	1.030	+ 1.016	-0.0955	+0.0866	-0.104
0.16340	0.17194	0.16761	20.645	0.0616	0.877	+ 0.866	-0.0590	+0.0804	-0.0951
0.17194	0.18082	0.17632	17.486	0.0574	0.743	+ 0.733	-0.0302	+0.0739	-0.0865
0.18082	0.19005	0.18537	14.679	0.0543	0.626	+ 0.617	-0.0081	+0.0673	-0.0780
0.19005	0.19965	0.19478	12.291	0.0504	0.524	+ 0.515	+0.0052	+0.0606	-0.0697

# Backup slide – TOTEM upgrade plans

## Timing Detector Development for Medium Pileup ( $\beta^* = 90$ m Runs)

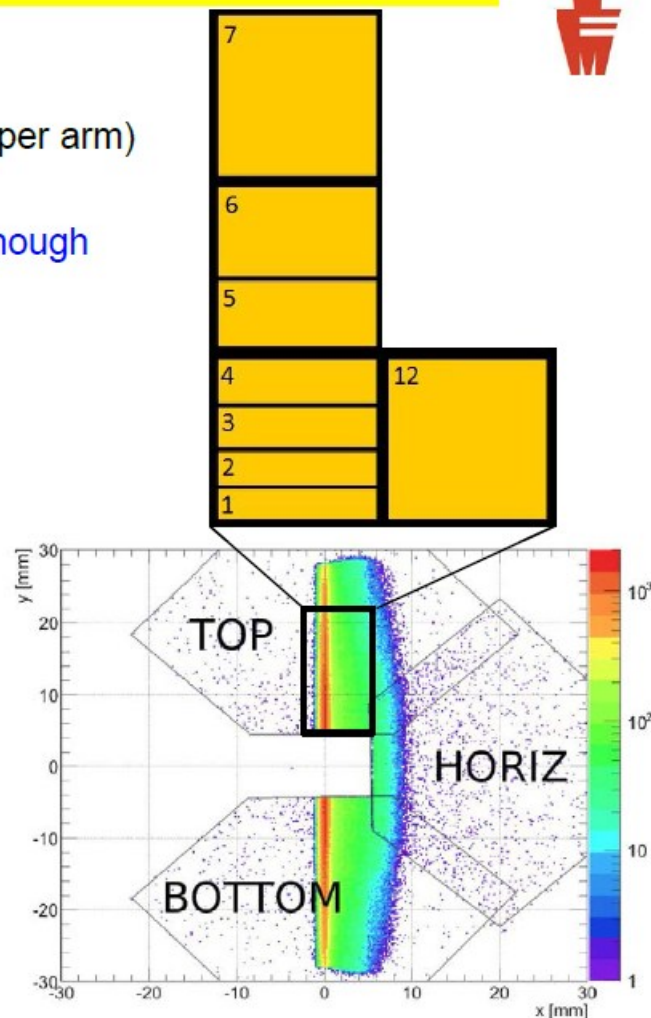
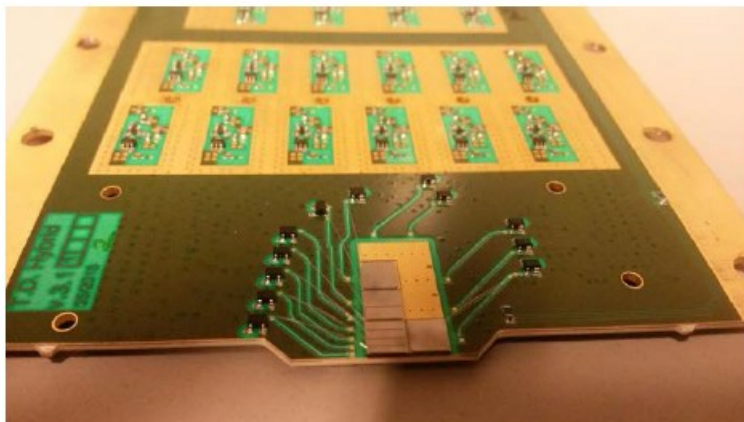


### Objective:

- 3 timing detector planes in 4 vertical RPs (1 pot pair per arm)
- Detector installation in Technical Stop 3 – YETS
- $\sim 60$  ps resolution per arm ( $\sim 100$  ps per detector) enough since at 90m the pileup  $\mu < 0.6$   
(different for CT-PPS:  $\beta^*=0.8$ m:  $\mu \leq 50$  !  
→ needs time resolution  $\sim 10$  ps)

### Development of Diamond Detectors:

Segmentation follows the diffractive hit distribution:  
almost constant occupancy per pixel



# Backup slide – theory interpretations

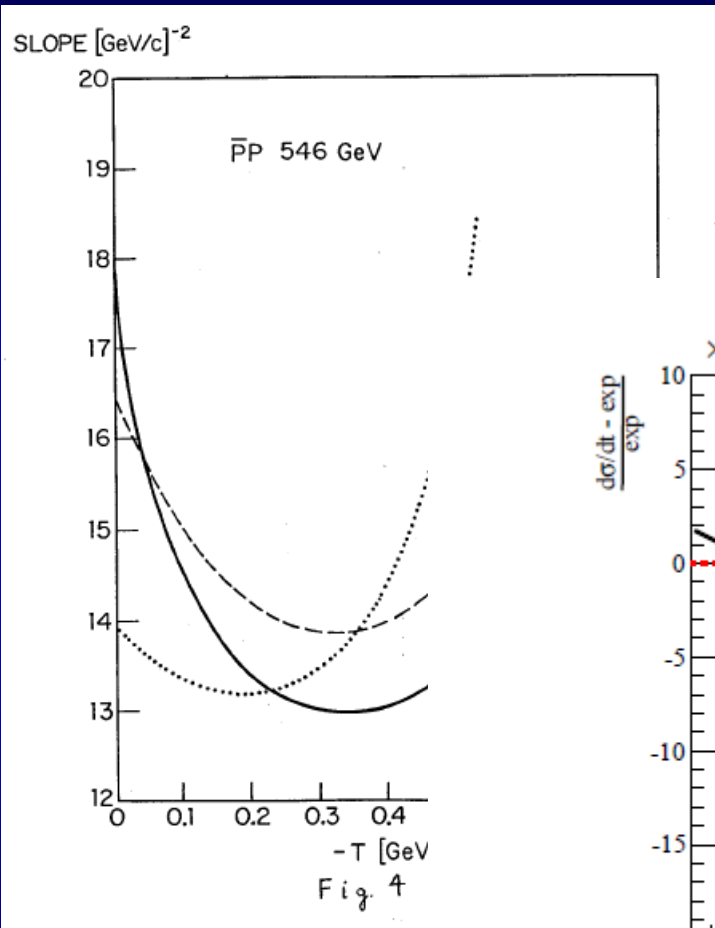
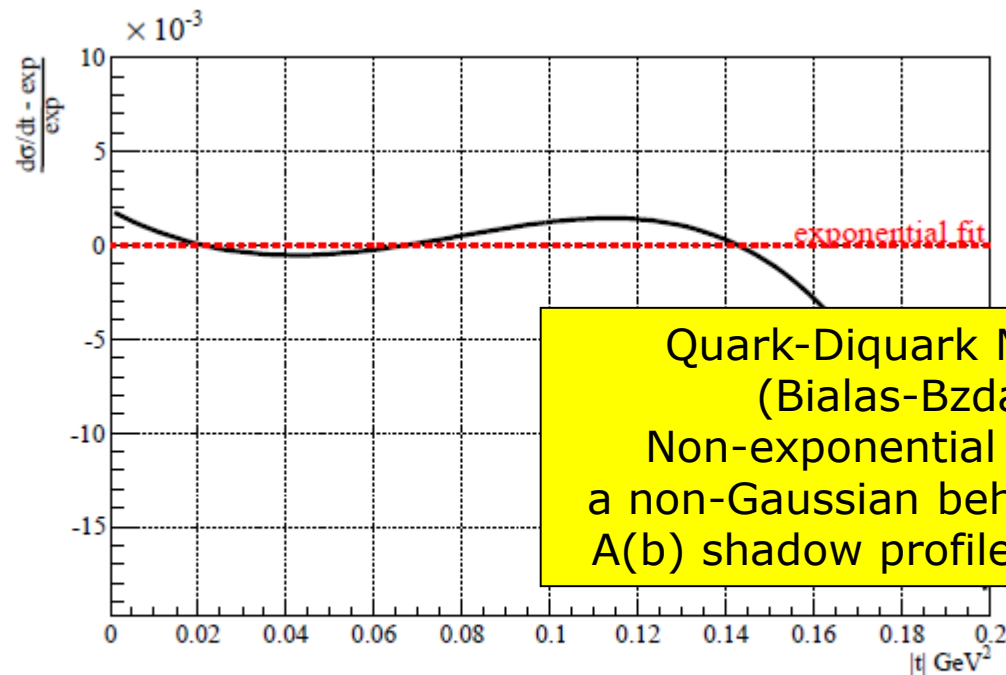


Figure 4 from  
Glauber-Velasco  
PLB 147 (1984) 380  
Slope is not quite  
Exponential:

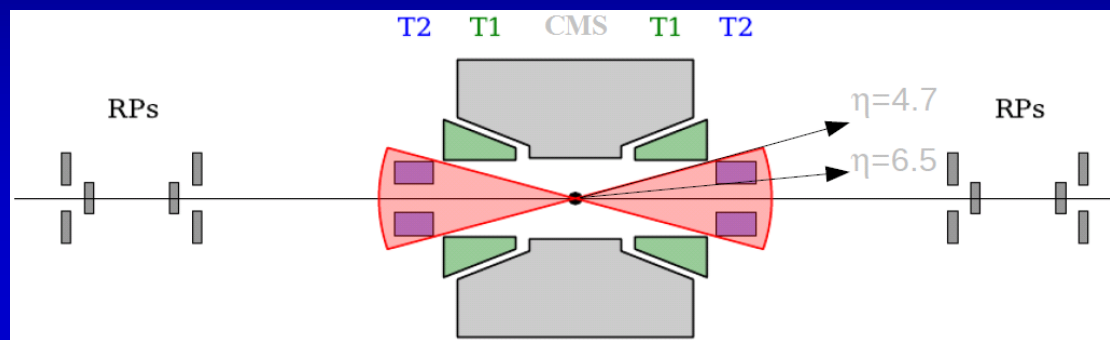


Quark-Diquark Models  
(Bialas-Bzdak)  
Non-exponential  $d\sigma/dt$ :  
a non-Gaussian behaviour of  
 $A(b)$  shadow profile function

Fig. 5. The ReBB model, fitted in the  $0.0 \leq |t| \leq 0.36 \text{ GeV}^2$  range, with respect to the exponential fit of Eq. (33). In the plot only the  $0.0 \leq |t| \leq 0.2 \text{ GeV}^2$  range is shown. The curve indicates a significant deviation from the simple exponential at low  $|t|$  values.

# TOTEM for double diffraction

**Aim:** Measurement of soft double diffractive cross section with particle  $\eta_{\min}$  visible to TOTEM T2 ( $4.7 < |\eta_{\min}| < 6.5$ ).  $\longrightarrow$   $\sigma_{DD}(|\eta_{\min}|)$  for  $3.4 < M_{DIFF} < 8$  GeV



**Event selection:** Trigger with T2, at least one track in both T2 hemispheres, no tracks in T1 “(0T1+2T2) topology”.

- ND background estimated scaling the MC prediction using a control sample from data dominated by ND (2T1+2T2 events)
- SD background estimated completely from data using a SD-dominated control sample (0T1+1T2) with protons in the RP

# TOTEM results on double diffraction

Phys. Rev. Lett. 111, 262001

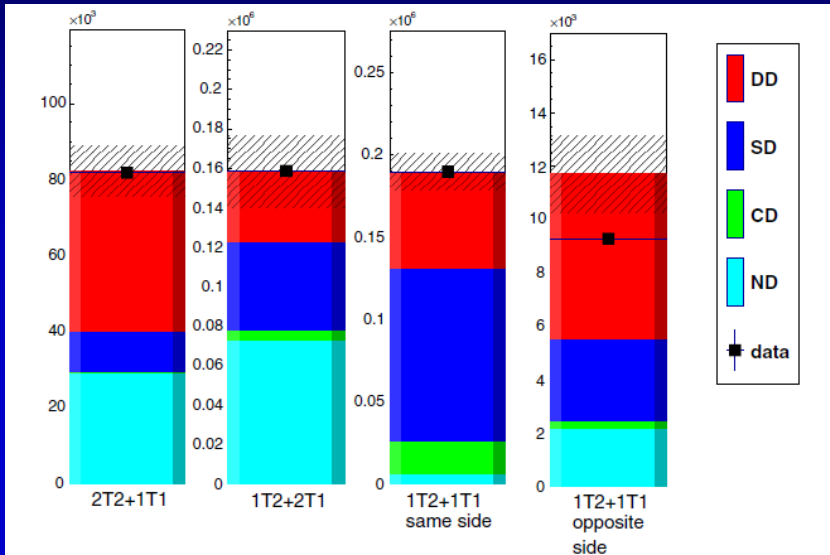


FIG. 1 (color online). Validation of background estimates for the full selection  $I_{\text{track}}$ . Each plot shows the corrected number of events in data (black squares) and the combined estimate with background uncertainties. The combined estimate is the sum of all components, from bottom to top: the ND estimate (cyan), CD estimate (green), SD estimate (blue), and DD estimate (red).

$$\sigma_{\text{DD}} = \frac{E(N_{\text{data}}^{2T2+0T1} - N_{\text{bckg}}^{2T2+0T1})}{\mathcal{L}},$$

E: experimental correction includes acceptance, tracking, reconstruction efficiencies (T2) and for only neutrals in T2

$$E = 0.9 \pm 0.1$$

$$\mathcal{L} = 40.1 \pm 1.6 \mu\text{b}^{-1}$$

TOTEM result:

$$\sigma_{\text{DD}} = 116 \pm 25 \mu\text{b}$$

$$4.7 < |\eta|_{\text{min}} < 6.5$$

for both diffractive systems

# TOTEM for double diffraction

TABLE III. Double diffractive cross-section measurements ( $\mu\text{b}$ ) in the forward region. Both visible and  $\eta_{\min}$  corrected cross sections are given. The latter is compared to PYTHIA and PHOJET predictions. PYTHIA estimate for total  $\sigma_{\text{DD}} = 8.1 \text{ mb}$  and PHOJET estimate  $\sigma_{\text{DD}} = 3.9 \text{ mb}$ .

	$I_{\text{track}}$	$D11_{\text{track}}$	$D22_{\text{track}}$	$D12_{\text{track}}$	$D21_{\text{track}}$
Visible	$131 \pm 22$	$58 \pm 14$	$20 \pm 8$	$31 \pm 5$	$34 \pm 5$
	$I$	$D11$	$D22$	$D12$	$D21$
$\eta_{\min}$	$116 \pm 25$	$65 \pm 20$	$12 \pm 5$	$26 \pm 5$	$27 \pm 5$
PYTHIA $\eta_{\min}$	159	70	17	36	36
PHOJET $\eta_{\min}$	101	44	12	23	23

TABLE IV. Summary of statistical and systematic uncertainties ( $\mu\text{b}$ ).

	$I$	$D11$	$D22$	$D12$	$D21$
Statistical	1.5	1.1	0.7	0.9	0.9
Background estimate	9.0	6.0	3.5	2.7	2.2
Trigger efficiency	2.1	1.2	1.0	0.9	0.9
Pileup correction	2.4	2.1	0.4	1.1	1.0
$T1$ multiplicity	7.0	3.9	0.7	1.6	1.7
Luminosity	4.7	2.6	0.5	1.1	1.1
Experimental correction	14.7	14.1	2.6	2.0	2.0
$\eta_{\min}$	15.4	11.0	1.5	2.9	2.9
Total uncertainty	24.8	19.6	4.8	5.1	4.9

Event categories:

I:  $|\eta|_{\min}$  corrected

D11:

$$4.7 < |\eta^{\pm}|_{\min} < 5.9$$

D22:

$$5.9 < |\eta^{\pm}|_{\min} < 6.5$$

SD & DD results combined  
seems to indicate  
factorisation breaking:

$$\sigma_{\text{DD}} (4.7 \leq |\eta_{\min}| \leq 6.5) \gg$$

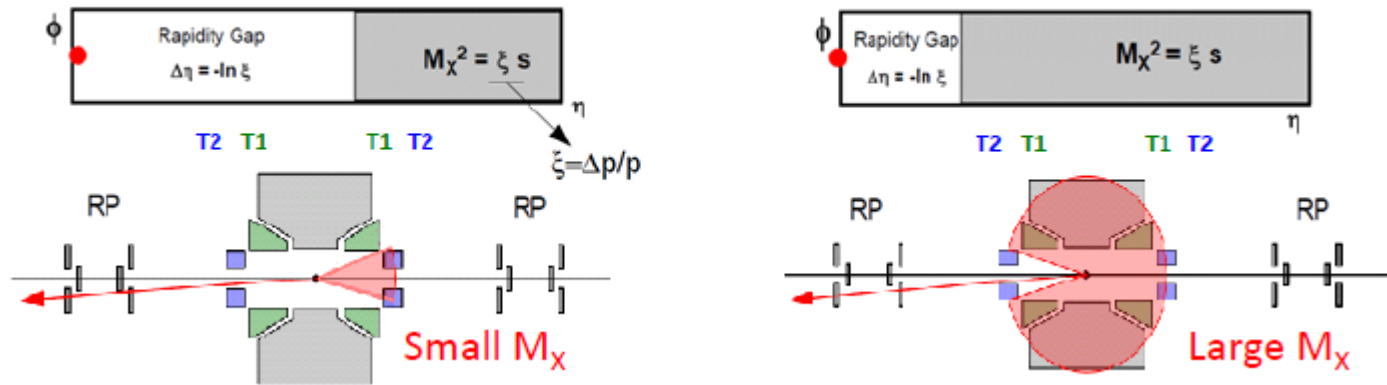
$$\sigma_{\text{SD}} (-4.7 \geq \eta_{\min} \geq -6.5) \times$$

$$\sigma_{\text{SD}} (4.7 \leq \eta_{\min} \leq 6.5) / \sigma_{\text{elastic}}$$

Note:  $|\eta|_{\min}$  correction:  
the dominant source of the  
uncertainty

# TOTEM for single diffraction

Rapidity gap ( $\Delta\eta = -\ln \xi$ ) determines diffractive mass ( $M_X^2 = \xi s$ )



Event classification based on tracks in T1 & T2, proton in RP

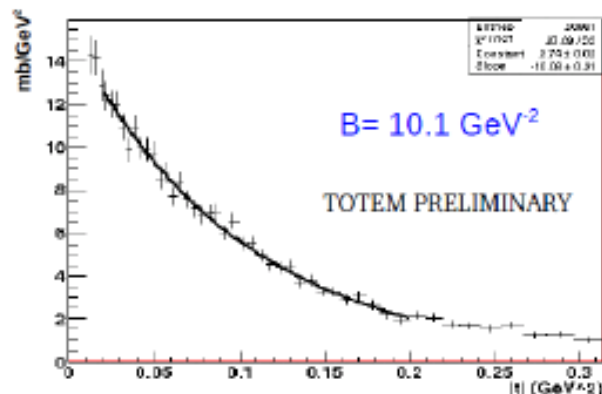
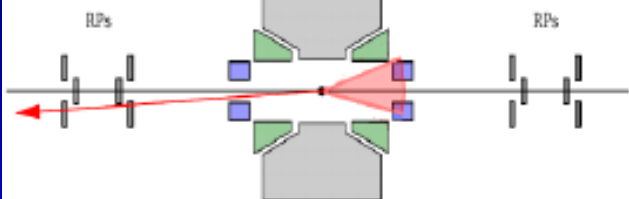
SD class	Configuration	$M_X$ [GeV]	$\xi = \Delta p/p$
Low mass	1 RP + opp. T2	3.4 – 8	$2 \times 10^{-7} - 10^{-6}$
Medium mass	1 RP + opp. T2 + opp. T1	8 – 350	$10^{-6} - 0.0025$
High mass	1 RP + opp. T2 + same T1	350 – 1100	0.0025 – 0.025
Very high mass	1 RP + both T2	1100 – ...	0.025 – ...

# TOTEM on single diffraction, 7 TeV

## Low Mass

$M=3.4 - 7 \text{ GeV}$

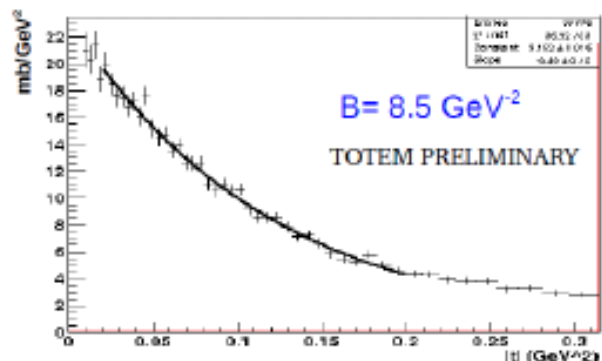
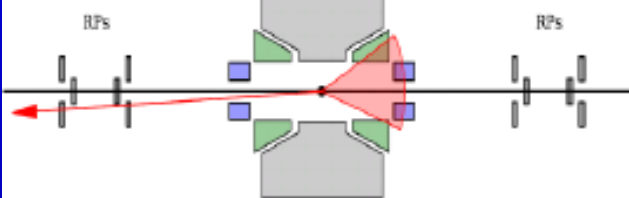
T2 T1 T1 T2



## Medium Mass

$M=7 - 350 \text{ GeV}$

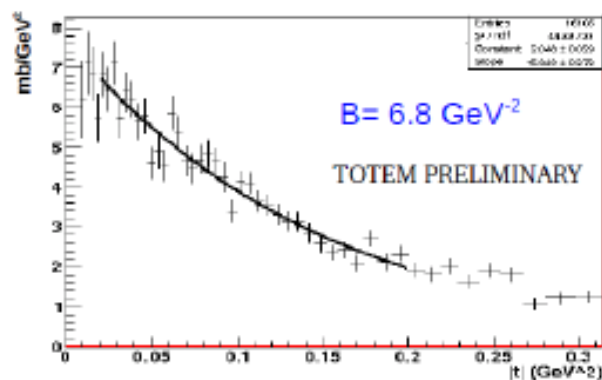
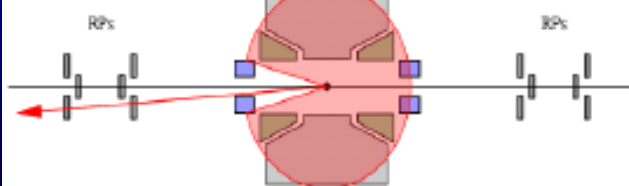
T2 T1 T1 T2



## High Mass

$M=0.35 - 1.1 \text{ TeV}$

T2 T1 T1 T2



### Corrections included:

- Trigger efficiency
- Proton acceptance & reconstruction efficiency
- Background subtraction
- Extrapolation to  $t = 0$

### Missing corrections:

- Class migration
- $\xi$  resolution & beam divergence effects

### Estimated uncertainties:

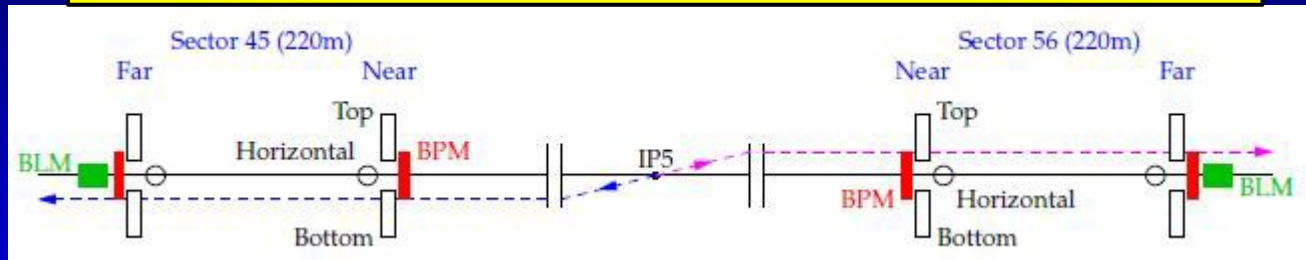
$B \sim 15\%$  ;  $\sigma \sim 20\%$

TOTEM preliminary:

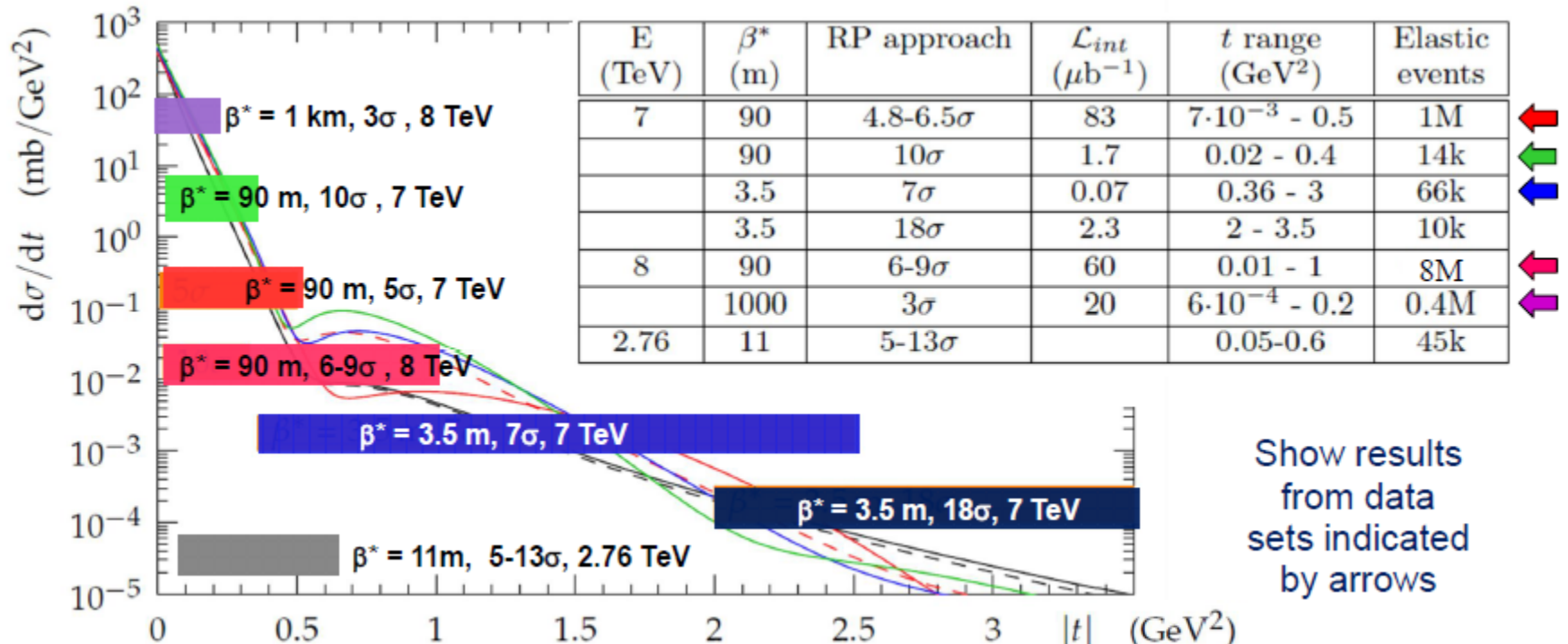
$\sigma_{SD} = 6.5 \pm 1.3 \text{ mb}$   
 $3.4 \text{ GeV} < M_{\text{diff}} < 1.1 \text{ TeV}$

# Event selection, data sets

Selected based on topology, low  $|\xi|$ , collinearity, & vertex .  
Key issues: RP alignment and optics.



Data sets at different conditions to measure elastics over wide  $t$ -range including very low  $|t|$



# 3 methods to measure $\sigma_{tot}$

elastic only  
(T1, T2 independent)

$$\sigma_{tot}^2 = \frac{16\pi}{(1 + \rho^2)} \frac{1}{\mathcal{L}} \left( \frac{dN_{el}}{dt} \right)_{t=0}$$

$\rho$  independent

$$\sigma_{tot} = \sigma_{el} + \sigma_{inel}$$

$L$  independent

$$\sigma_{tot} = \frac{16\pi}{(1 + \rho^2)} \frac{(dN_{el}/dt)_{t=0}}{(N_{el} + N_{inel})}$$

7 TeV

$$\sigma_{TOT} = 98.3 \text{ mb} \pm 2.0 \text{ mb}$$

EPL 96 (2011) 21002

$$\sigma_{TOT} = 98.6 \text{ mb} \pm 2.3 \text{ mb}$$

EPL 101 (2013) 21002

$$\sigma_{TOT} = 99.1 \text{ mb} \pm 4.3 \text{ mb}$$

EPL 101 (2013) 21004

$$\sigma_{TOT} = 98.1 \text{ mb} \pm 2.4 \text{ mb}$$

EPL 101 (2013) 21004

8 TeV: PRL 111, 012001

$$\sigma_{TOT} = 101.7 \text{ mb} \pm 2.9 \text{ mb}$$

# TOTEM total cross-section results

7 TeV

*elastic observables only:*

$$\sigma_{\text{tot}}^2 = \frac{16\pi}{1 + \rho^2} \frac{1}{\mathcal{L}} \left. \frac{dN_{\text{el}}}{dt} \right|_0 \quad (\rho=0.14 \text{ [COMPETE extrapol.]})$$

test validity of  
optical theorem  
at ~3.5 % level

June 2011 (EPL96):  $\sigma_{\text{tot}} = (98.3 \pm 2.8) \text{ mb}$

Oct. 2011 (EPL101):  $\sigma_{\text{tot}} = (98.6 \pm 2.2) \text{ mb}$

different beam intensities !

$\sigma_{\text{tot}}$

*q independent:*

$$\sigma_{\text{tot}} = \frac{1}{\mathcal{L}} (N_{\text{el}} + N_{\text{inel}})$$

$$\sigma_{\text{tot}} = (99.1 \pm 4.3) \text{ mb}$$

*luminosity independent:*

$$\sigma_{\text{tot}} = \frac{16\pi}{1 + \rho^2} \frac{dN_{\text{el}}/dt|_0}{N_{\text{el}} + N_{\text{inel}}}$$

$$\sigma_{\text{tot}} = (98.0 \pm 2.5) \text{ mb}$$

First measurements of the total proton-proton cross section at the LHC energy of  $\sqrt{s} = 7 \text{ TeV}$   
[EPL 96 (2011) 21002]

Measurement of proton-proton elastic scattering and total cross-section at  $\sqrt{s} = 7 \text{ TeV}$   
[EPL 101 (2013) 21002]

Measurement of proton-proton inelastic scattering cross-section at  $\sqrt{s} = 7 \text{ TeV}$   
[EPL 101 (2013) 21003]

Luminosity-independent measurements of total, elastic and inelastic cross-sections at  $\sqrt{s} = 7 \text{ TeV}$   
[EPL 101 (2013) 21004]

A luminosity-independent measurement of the proton-proton total cross-section at  $\sqrt{s} = 8 \text{ TeV}$   
[Phys. Rev. Lett. 111, 012001 (2013)]

# TOTEM total cross-section @ 8TeV with luminosity-independent method

TABLE I. Description of the available data samples. The RP position is given as the RP approach to the beam in multiples of the transverse beam size ( $\sigma_{\text{beam}} \sim 0.7$  mm). The third column shows the lowest  $|t|$  values reached in the elastic sample after all cuts. The last two columns show the number of elastic and inelastic events collected.

Data set	RP position	$ t _{\text{min}}$ (GeV <sup>2</sup> )	Elastic events	Inelastic events
1	$6.0\sigma_{\text{beam}}$	0.01	$416 \times 10^3$	$2.30 \times 10^6$
2	$9.5\sigma_{\text{beam}}$	0.02	$238 \times 10^3$	$1.72 \times 10^6$

Needs precise control of LHC imperfections and recalibration from data at IP5:

$$\beta^* = 90\text{m},$$

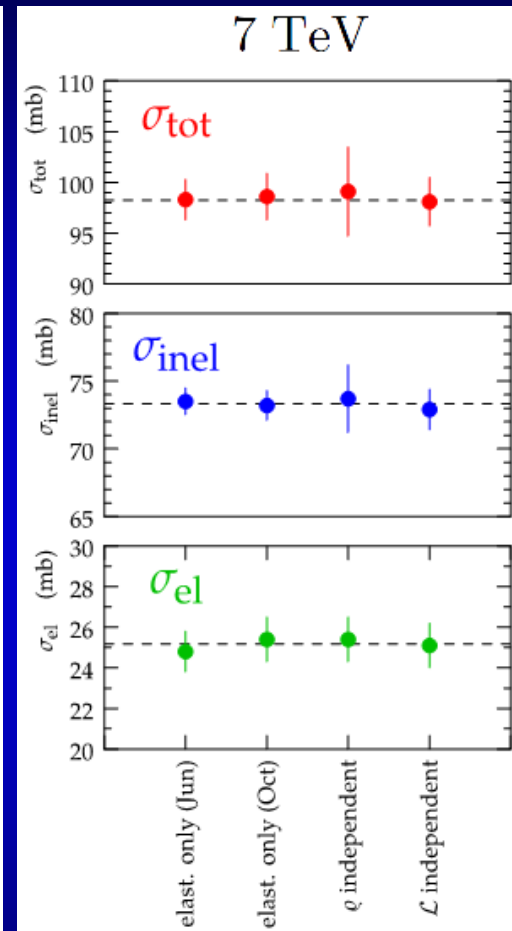
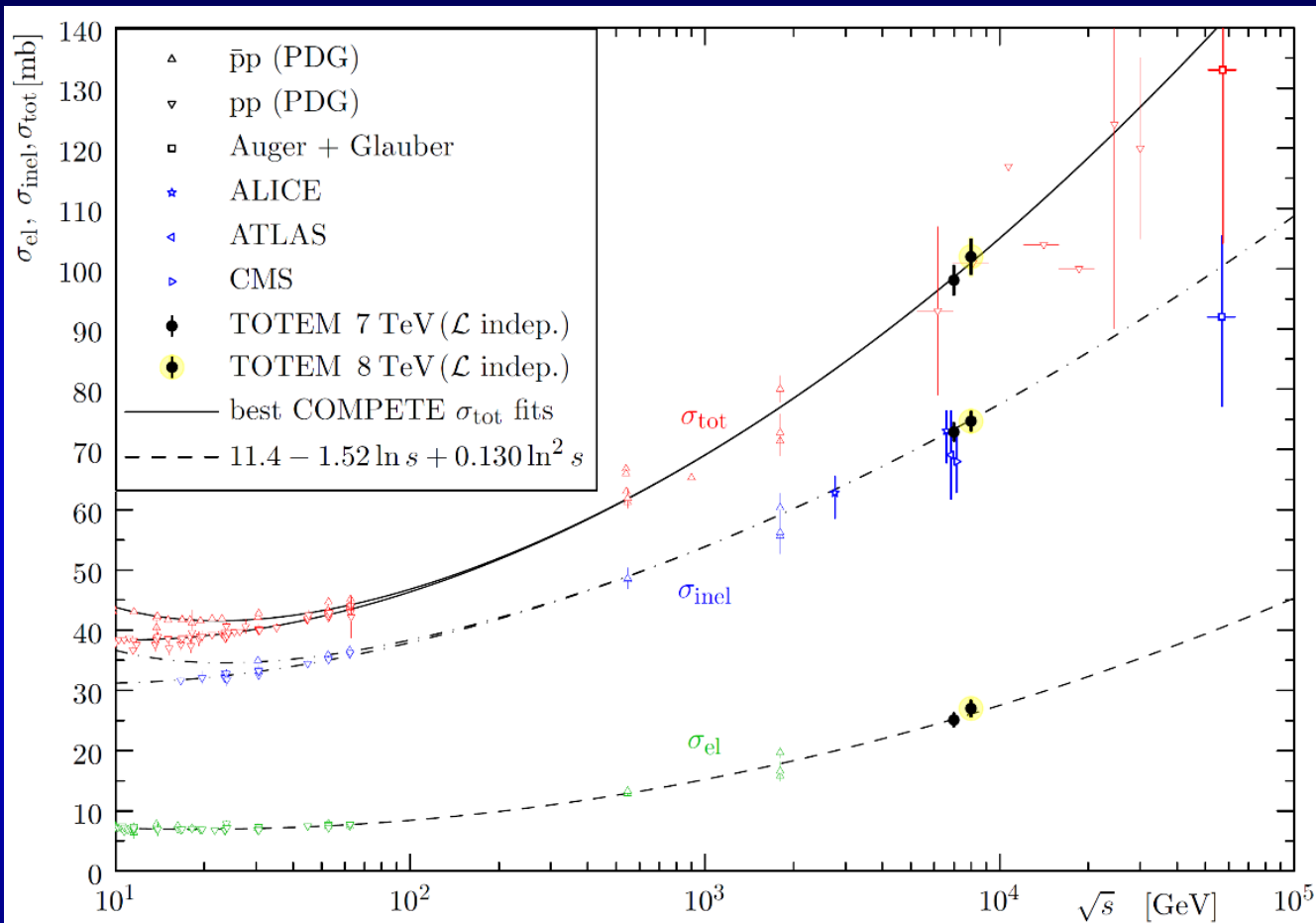
optics error reduction by 2-10,

[arXiv:1406.0546](https://arxiv.org/abs/1406.0546)

TABLE II. Overview of the analysis steps, associated corrections, and systematic uncertainties to the differential and total elastic rate.

Source	Effect on	$ t  = 0.01$ GeV <sup>2</sup>	0.1 GeV <sup>2</sup>	0.2 GeV <sup>2</sup>
Alignment	$t$	$\pm 0.21\%$	$\pm 0.3\%$	$\pm 0.57\%$
Kinematics reconstruction: Optics, beam energy	$t$	$\pm 1.09\%$	$\pm 0.72\%$	$\pm 4.3\%$
Selection	norm.		$\pm 0.5\%$	
Acceptance (correction factor)	$dN/dt$	$3.3 \pm 0.024$	$1.2 \pm 0.002$	$1.8 \pm 0.004$
Resolution unfolding	$t$	$(0.5 \pm 0.1)\%$	$(-0.2 \pm 0.003)\%$	$(-2.6 \pm 0.1)\%$
Efficiency	norm.	Uncorrelated inefficiency: $(10 \pm 0.6)\%$		
		Correlated inefficiency: $(3 \pm 1)\%$		
		Pileup: $(4.7 \pm 0.4)\%$		
Extrapolation/Fit		$\frac{dN_{\text{el}}/dt _{t=0}}{B}$	$\pm 2.5\%$	$(19.9 \pm 0.3) \text{ GeV}^{-2}$

# TOTEM: total cross-sections



7 TeV: Excellent agreements between different methods.  
 Ongoing analysis for 8 and 2.6 TeV with different optics/methods.